POTASSIUM CURRENTS AND CONDUCTANCE

COMPARISON BETWEEN MOTOR AND SENSORY MYELINATED FIBERS

Y. PALTI, N. MORAN, AND R. STÄMPFLI, *Department of Physiology and Biophysics, Faculty of Medicine–Technion, Haifa, Israel*

ABSTRACT The potassium conductance system of sensory and motor fibers from the frog *Rana esculenta* were studied and compared by means of the voltage clamp. The potassium ion accumulation was first estimated from the currents and reversal potentials within the framework of both a three-compartment model and diffusion-in-an-unstirred-layer model. The potassium conductance parameters were then computed using the measured currents and corrected ionic driving forces. It was found that the potassium accumulation is faster and more pronounced in sensory fibers, the voltage dependency of the potassium conductance is steeper in sensory fibers, the maximal potassium conductance, corrected for accumulation, is ~1.1 S/cm^2 in sensory and 0.55 S/cm^2 in motor fibers, and that the conductance time constants, τ_n, are smaller in sensory than in motor fibers. These differences, which increase progressively with depolarization, are not detectable for depolarizations of 50 mV or smaller. The interpretation of these findings in terms of different types of potassium channels as well as their implications with regard to the differences between the excitability phenomena in motor and sensory fibers are discussed.

Myelinated nerve fibers are functionally separable into two distinct groups, sensory and motor. The major differences between the two groups are: (*a*) Sensory fibers fire repetitively while motor fibers fire only once in response to a prolonged stimulus. (Stämpfli and Hille, 1976), and (*b*) The initial rate of decline (repolarization) of the action potential of motor fibers is slow compared with sensory fibers. This rate increases to roughly the "sensory" value about halfway along the repolarization phase. The difference between the physiological properties can be exemplified by applying tetraethylammonium (TEA) which prolongs the duration of the action potential primarily in motor fibers (Schmidt and Stämpfli, 1964, 1966, Bergman and Stämpfli, 1966).

While the specialized function of these two groups is well understood, little is known about the differences between their basic mechanisms of excitability. There is reason to believe that the behavioral difference between the two types of fibers is due, at least in part, to the difference in their potassium conductance systems. The main piece of evidence regarding the difference between the potassium conductance systems comes from the work of Bretag and Stämpfli (1975). Their two major experimental findings were: a shift of the n_∞ vs. voltage relationship on the voltage axis, and a difference in the voltage dependency of the sensory and motor current time constants. Thus, the $\tau_{motor}/\tau_{sensory}$ ratio progressively increases with membrane potentials, for depolarizations higher than 70 mV.

Dr. Stämpfli's address is the First Physiological Institute, Saarland University, Homburg, West Germany.

However, these results were obtained in fibers internally perfused by 110 mM KCl (plus 10 mM NaCl) and externally bathed in 117 mM KCl Ringer's. Since these experimental conditions are far from natural (as far as ionic composition and resting potential are concerned) and because of the rather limited potential range studied, it is the purpose of this work to further compare the potassium conductance system of sensory and motor fibers. The study will include the comparative determination of (*a*) potassium conductance in both preparations under comparable conditions as a function of both voltage and time and (*b*) the potassium ion accumulation during membrane depolarization.

METHODS

Experimental

Motor and sensory myelinated fibers were dissected from the sciatic nerve of the frog *Rand esculenta* as described by Stämpfli (1969) (see also Stämpfli and Hille, 1976), and voltage clamped using the mounting procedure and apparatus described by Nonner (1969).

The node was externally perfused with Ringer's solution containing 60–300 nM tetrodotoxin (TTX). The internal ionic composition was controlled by cutting the fibers short (300–600 μm) in 117 mM KCl. The pH was adjusted to 7.4 by Tris buffer. Temperature was held constant at 15°C.

The command voltage pulses were generated by a D/A converter under computer program control. Membrane currents were filtered by a 40 KHz low-pass filter and sampled at 20-μs intervals by means of a 10-bit A/D converter operating also under program control.

Two series of pulses were used: (*a*) Single depolarizing pulses for the determination of both the *I-V* relationship and the time course of potassium currents (Bretag and Stämpfli, 1975); these pulses ranged between 10 and 150 mV in steps of 10 mV. (*b*) Double pulses, which generated "tail currents," for the determination of potassium reversal potential, V_K, as a function of prepulse amplitude, V_{pp}, and duration, t_{pp} (Moran et al., 1980), as illustrated in Fig. 2 *A*.

The resting leakage conductance, G_L, was determined by means of single, -24 to -60 mV, hyperpolarizing pulses. Leakage current was computed using the measured G_L assuming a linear current-voltage relationship that crosses the voltage axis at $V_L = 0$, i.e., at the resting potential. (All potentials are given relative to the resting potential, depolarization is positive, while hyperpolarization is in the negative direction.) Note that in the computation of potassium ion accumulation (Moran et al., 1980) I_L was not subtracted from I_K as a major fraction of it is carried by potassium ions.

The node was held in its resting potential value, V_H, in between voltage clamp pulses during V_K determination. When *I-V* relationships were determined the membrane was held at -30 mV, in all but four fibers (4673, 4773, 7877, 7977).

At the end of each experiment the node was destroyed by a strong hyperpolarization and the absolute membrane potential, E_M was determined.

Analytical

CALCULATION OF STEADY STATE V_K SHIFTS The steady-state concentration of potassium at the outer surface of the membrane, i.e., in the so-called "space," $[K_s]$, was calculated on the basis of the total steady state potassium currents, $I_{K_{ss}}$, at each depolarization. The current density has been calculated using the measured fiber length under the following assumptions: the axoplasmic resistance is 110 Ω cm, the node area is 50 μm^2 (Nonner et al., 1975) and the fiber diameter is 11 μm (an average diameter of 12 motor fibers), a value representative of both motor and sensory fiber diameters. (Such a similarity was reported by Stämpfli and Hille, 1976.)

Note, that since leakage current, I_L, in the frog is believed to be carried mainly by potassium ions (Hille, 1973), I_L was included in the potassium current whenever $[K_s]$ was computed or determined experimentally.

The calculation was done using the equation formulated within the framework of a three-compartment model for steady-state accumulation (Eq. 2 of Moran et al., 1980) in a rearranged form:

$$[K_s] = [K_o] + (1 + [K_o]/\Sigma[\text{ions}])/(F \cdot P_{K_{ss}}/I_{K_{ss}} + 1/\Sigma[\text{ions}]) \quad (1)$$

where F is the Faraday constant, Σ[ions] is the sum of activities of electrical charge carriers in the space, $[K_o]$ is the K^+ concentration in the bulk solution, and $P_{K_{ss}}$ is the apparent permeability of the barrier externally delimitating the space, as determined from steady-state values of current and accumulation.

The $P_{K_{ss}}$ values were shown to be significantly smaller for small depolarizations (+40, +50 mV) than for higher ones (Moran et al., 1980). Therefore, the averaged values of $P_{K_{ss}}$ determined at +70 and +100 mV for each fiber (Table II), were used for the $[K_s]$ calculation for depolarizations higher than +50 mV, whereas for smaller depolarizations the values of $P_{K_{ss}}$ determined at +40 mV were used. (For technical reasons, only single values of $P_{K_{ss}}$, determined at +150 mV, were used for fibers 7877 and 7977 throughout the whole range of membrane potentials.) The computed $[K_s]$ for all potentials were converted to V_Ks by means of the Nernst relationship, assuming a constant internal potassium concentration of 117 mM.

CORRECTION FOR LEAKAGE CURRENT Leakage current, I_L, was subtracted from all currents before the calculation of potassium chord conductance, G_K, assuming ohmic leakage conductance. I_L was calculated by either of the following two methods: (*a*) For calculation of G_K in cases where V_K shifts were ignored, it was assumed that $V_L = 0$. (*b*) Whenever V_K shifts were taken into account in a computation of G_K, they were also introduced into the calculation of I_L. This was done under the following assumptions: (*a*) outward I_L is carried only by potassium ions ($[Na_{in}] \rightarrow 0$), (*b*) the I_L-V_M relationship is linear, and (*c*) all reversal potentials are adequately described by the Goldman equation.

CALCULATION OF τ_n The time constant of the potassium conductance, τ_n, was determined from the exponential segments of the time course of G_K, using the relation:

$$\ln \frac{n_\infty - n_t}{n_\infty - n_0} = -t/\tau_n, \quad (2)$$

n_t being the potassium conductance parameter at any time t, and the subscripts o and ∞ denoting the n values at the onset and at the termination of a long depolarizing pulse. The values of $n_\infty - n_t$ were determined from the potassium current by means of the following equation:

$$n_\infty - n_t = \left(\frac{1}{\bar{G}_K}\right)^{1/4} \{[I_{K_\infty}/(V_M - V_{K_\infty})]^{1/4} - [I_{K_t}/(V_M - V_{K_t})]^{1/4}\}. \quad (3)$$

The power of 4 for n was adopted following Koppenhoffer (1967) and Koppenhoffer and Schmidt (1968 *a* and *b*), and Dodge (1961, 1963) who used it for *Xenopus laevis* and *Rana pipiens*, respectively. For any given depolarization the maximal potassium conductance, $\bar{G}_K$, as well as $n_\infty - n_0$ are constant and therefore need not be known for the determination of τ_n. The slope of $\ln (n_\infty - n_t)$ vs. time was determined within the first 2 ms and the first 6 ms of the depolarization for sensory and motor fibers, respectively.

RESULTS

I-V Relationships

Steady-state current-voltage relationships (corrected for leakage) obtained from six motor and seven sensory fibers are shown in Fig. 1 *A*. The fibers evidently fall into two distinct groups. The averaged current values (±SEM) for each type of fibers are given in Fig. 1 *B*. For small depolarizations (<60 mV) the *I-V* curves of both types of fibers practically superimpose. The difference becomes evident at membrane depolarizations higher than +60 mV, where the

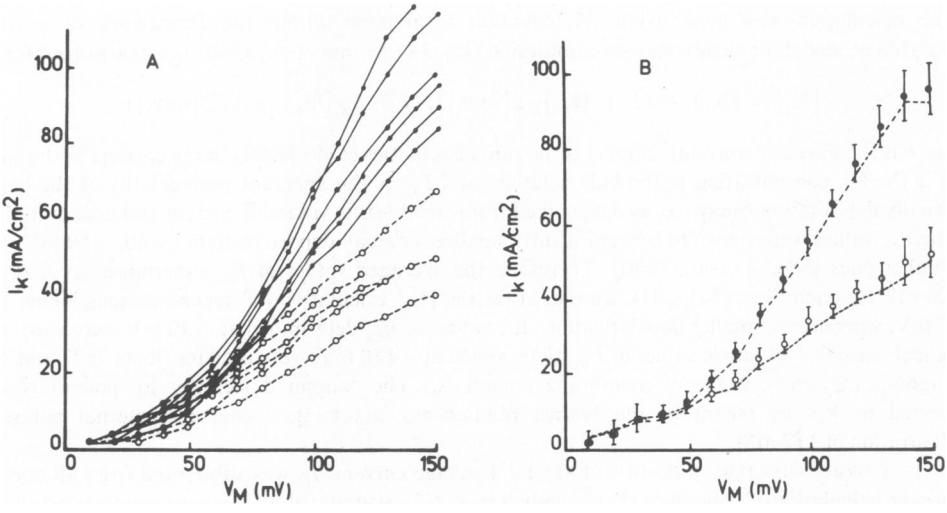

FIGURE 1 Steady-state potassium current-voltage relationships. Motor fibers, open circles; sensory fibres, filled circles. (*A*) *I-V* curves plotted for each individual fiber separately. (*B*) The mean (±SEM) currents, averaged for each fiber type separately vs. membrane potential. The potassium currents were corrected for leakage under either of the following two assumptions: (*a*) leakage reversal potential, V_L, varies with V_K (symbols) or (*b*) $V_L = 0$ at all membrane potentials (dotted line).

steady-state outward potassium current in the sensory fibers, I_K^s, becomes progressively larger when compared with the current in motor fibers, I_K^m. At depolarizations of 150 mV the ratio I_K^s/I_K^m approaches 2.

This result is not affected by the mode of leakage current correction, i.e., whether a constant leakage reversal potential, V_L (Fig. 1 *B*, dotted line), or a V_L varying with V_K is introduced into the I_L computation (Fig. 1 *A* and *B*, symbols). However, since leakage current is believed to be mainly carried by potassium ions (Hille, 1973), the procedure of leakage correction using V_L varying with V_K was generally adopted (see Methods).

To translate the above potassium currents into conductances the ion driving force ($V_M - V_K$) has to be known. However, since potassium ions accumulation seems to be different in motor and sensory fibers (Moran et al., 1980), to properly compare the conductance systems of the two, the potassium accumulation had to be evaluated and eliminated.

K^+ Accumulation in Sensory and Motor Fibers

Fig. 2 *A* shows instantaneous *I-V* curves obtained from four motor and seven sensory fibers, after a 100 mV depolarization lasting 5 ms. Each line was constructed on the basis of six instantaneous current points by the least mean squares method. The fit to a linear relationship was very good (Moran et al., 1980). The "sensory" instantaneous *I-V* relationships (continuous lines) and their zero-current crossover-points group separately from the "motor" instantaneous *I-V* curves (dashed lines) and crossover points, indicating that the V_K shifts are larger in the sensory fibers.

Note also, that the slopes of the instantaneous *I-V* curves, which are the measure of the chord conductance, are almost twice as large in the sensory, as compared with the motor fibers.

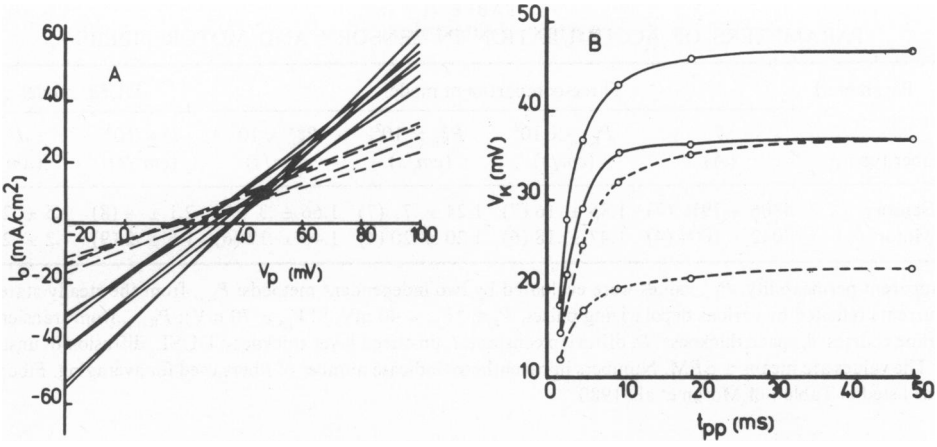

FIGURE 2 Potassium conductance and reversal potential, V_K, in motor and sensory fibers. (*A*) instantaneous potassium *I-V* relationships of individual fibers. Each line was constructed on the basis of a least mean square fit to the initial current elicited upon stepping membrane potential from a 100-mV, 5-ms depolarization to the following V_Ps: −20, 0, 20, 40, 60 (or 70), and 100 mV. Motor fibers, dashed lines; sensory fibers, continuous lines. The potential corresponding to the zero current-cross-over-point was taken as V_K. Note separate grouping of slopes and V_Ks corresponding to motor and sensory fibers. (*B*) The change of V_K with time during a 100-mV depolarization in two motor (open circles) and two sensory (filled circles) fibers. Lines fitted by eye to experimental zero-cross-over-points (see *A*).

Fig. 2 *B* illustrates the whole time course of the V_K shifts during a 100-mV depolarization for two motor (dashed lines) and two sensory fibers (continuous lines). The V_K shifts in sensory fibers are seen to be larger than those of the motor fibers throughout the duration of the depolarization.

Table I lists the average values of V_K shifts determined in the above 11 fibers of Fig. 1 *A* after 100-mV depolarizations lasting either 5 or 50 ms. Also listed are the corresponding concentrations of potassium obtained from the V_K values by the Nernst relationship.

From the table and figures it may be concluded that potassium ions accumulate to a lesser extent in motor as compared with sensory fibers. The parameters which describe the potassium accumulation in the external "space" within the framework of a three-compartment model have been analyzed by Moran et al. (1980). Table II lists the calculated

TABLE I

POTASSIUM REVERSAL POTENTIAL, V_K, AND ION CONCENTRATION IN THE SPACE [K_s] AS A FUNCTION OF THE DEPOLARIZING PULSE DURATION, t_{pp}, IN MOTOR AND SENSORY FIBERS

t_{pp}	5 ms		50 ms	
Fiber type	V_K (mV)	(K_s) (mM)	V_K (mV)	(K_s) (mM)
Sensory (7)	31.4 ± 2.0	24.6 ± 2.2	38.6 ± 2.2	33.0 ± 3.1
Motor (4)	19.6 ± 2.0	15.3 ± 1.3	28.0 ± 3.9	21.5 ± 3.7

The values are means ± SEM. Numbers in parentheses indicate number of fibers used for averaging.

TABLE II

PARAMETERS OF ACCUMULATION IN SENSORY AND MOTOR FIBERS

Parameters	Three-compartment model				DUSL model	
Fiber type	θ (Å)	$P_{K_{s(tr)}} \times 10^2$ (cm/s)	$P^{*}_{K_{ss}} \times 10^2$ (cm/s)	$P^{**}_{K_{ss}} \times 10^2$ (cm/s)	$D \times 10^6$ (cm^2/s)	l (μm)
Sensory	4806 ± 791 (7)	1.85 ± .16 (7)	1.24 ± .7 (7)	1.66 ± .3 (7)	2.1 ± .4 (8)	1.5 ± .2 (8)
Motor	7042 ± 1004 (4)	1.47 ± .18 (6)	1.20 ± .20 (4)	1.40 ± .17 (6)	1.6 ± .2 (9)	1.2 ± .2 (9)

The apparent permeability, P_{K_s}, values were evaluated by two independent methods: $P_{K_{ss}}$, from the steady-state V_Ks and currents (elicited by various depolarizing pulses, V_{pp}s: $^{*}V_{pp}$ = 40 mV, $^{**}V_{pp} \geq$ 70 mV); $P_{K_{s(tr)}}$, from transients in their time courses; θ, space thickness; D, diffusion constant; l, unstirred layer thickness; DUSL, diffusion in unstirred layer. The values are means ± SEM. Numbers in parentheses indicate number of fibers used for averaging. Fibers are same as listed in Table I of Moran et al., 1980.

parameters, namely, the space thickness, θ, and the external barrier permeability, P_{K_s}, averaged for six motor and seven sensory fibers.

The two types of fibers do not seem to differ in their P_{K_s} values, as determined either from the steady-state values of potassium current and accumulation, $P_{K_{ss}}$, or from the transients of accumulation and current, $P_{K_{s(tr)}}$ (see Moran et al., 1980).

In contrast, the average apparent space thickness, θ, seems to be significantly larger in motor as compared with sensory fibers: 7042 ± 1004 (SEM) vs. 4806 ± 791 (SEM) Å.

Contrary to the above, the two types of fibers do not seem to differ significantly when compared within the framework of the diffusion-in-an-unstirred-layer model of accumulation. The average values of the diffusion constant, D, and of the unstirred layer thickness, l, from eight sensory and nine motor fibers are listed in Table II.

Note, however, that some motor fibers (four out of the 20 motor fibers studied here) could not be included in this analysis, because they showed only negligible shifts of V_K during depolarizing pulses.

Leakage Conductance

The resting leakage conductances, G_L, calculated from currents elicited by hyperpolarizing pulses, were not significantly different in sensory and motor fibers. The average G_L values were 38.4 ± 2.7 and 42.7 ± 7.2 mS/cm^2 in the sensory and motor fibers, respectively.

Potassium Chord Conductance

Fig. 3 *A* depicts the average values (±SEM) of steady-state potassium chord conductance, G_{K_∞} as a function of membrane potential, V_M, in sensory (dots) and motor (circles) fibers. G_{K_∞} is defined by the relation

$$G_{K_\infty} = I_{K_\infty}/(V_M - V_K). \quad (4)$$

The points in Fig. 3 *A* were obtained after correcting the driving force in each fiber separately, for the K^+ accumulation (by calculating the V_K shifts at each membrane potential from the steady-state potassium current—see Methods). The values of chord conductance thus obtained are almost twice as large as those calculated under the assumption that the V_K shifts

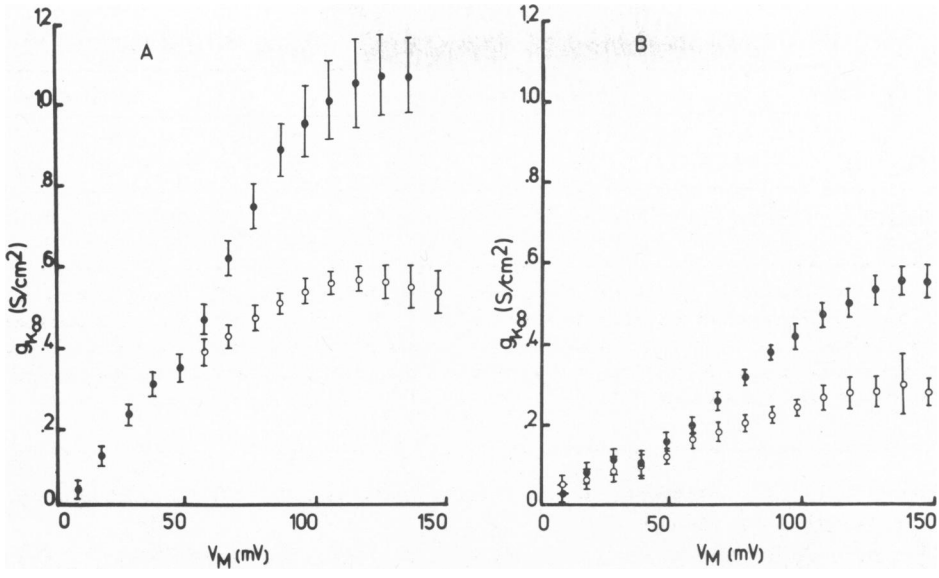

FIGURE 3 Potassium steady-state chord conductance, G_{K_∞}, as a function of membrane potential, V_M. Symbols: average G_{K_∞} ± SEM for six motor (open circles) and seven sensory (filled circles) fibers, calculated from: $G_{K_\infty}/(V_M - V_K)$. (*A*) G_{K_∞} values corrected for potassium accumulation. (*B*) G_{K_∞} values calculated assuming a constant $V_K = -25$ mV.

can be ignored, i.e., taking V_K as a constant (Fig. 3 *B*). Fig. 3 illustrates that for small depolarizations the change in nodal membrane potassium conductance with potential is similar in sensory and motor fibers. In contrast, during strong depolarizations (>50 mV) the potassium conductance of sensory fibers is progressively higher than that of motor fibers. At depolarization of 150 mV the potassium conductance of sensory fibers is about twice as large as that of motor fibers.

Fig. 4 *A* presents the motor and sensory steady-state $G_{K_\infty} - V_M$ curves of Fig. 3 *A*, normalized to their maximal values ($\bar{G}_K$). In Fig. 4 *B* the motor and sensory $n_\infty - V_M$ relationships are compared. n_∞ is calculated from:

$$n_\infty = (G_{K_\infty}/\bar{G}_K)^{1/4}. \tag{5}$$

The figure illustrates that the potassium conductances of motor and sensory fibers differ in their voltage dependence.

Conductance Kinetics

The potassium conductance kinetics were derived from the time course of potassium currents recorded during depolarizations of +70 mV and +150 mV, taking into account the time course of the V_K shifts. The shifts were calculated on the basis of the three-compartment-model equation (Moran et al., 1980), and the space parameters determined for each individual fiber. The initial value of V_K was taken as −25 mV, i.e., corresponding to $[K_s]$ in the bulk solution (2.5 mM).

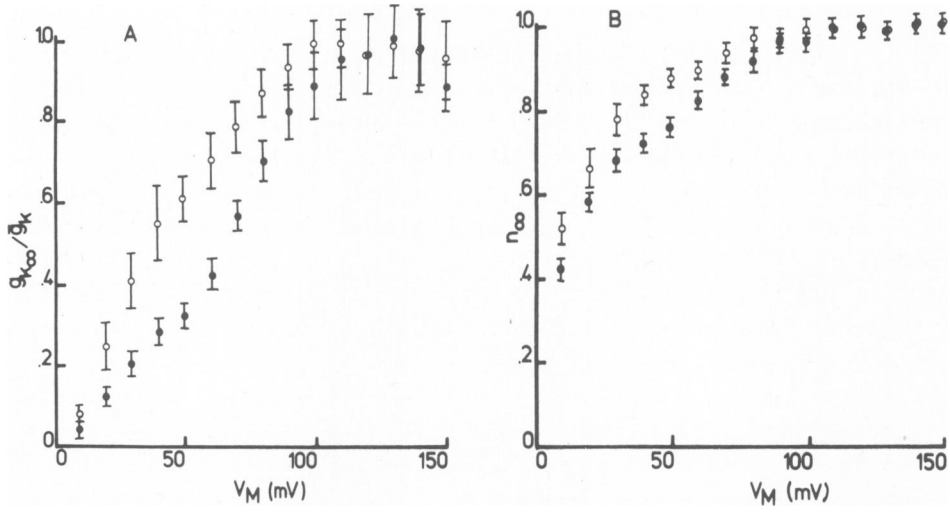

FIGURE 4 Normalized steady-state potassium chord conductance, n_∞, as a function of membrane potential, V_M. The values of n_∞ were calculated from: $(G_{K\infty}/G_K)^{1/x}$; (*A*) $x = 1$; (*B*) $x = 4$. Other details as in Fig. 3.

Table III lists the average values of τ_n obtained for seven sensory (τ_n^s) and six motor (τ_n^m) fibers at two depolarizations, 70 and 150 mV.

The potassium channels in motor fibers seem to be characterized by larger time constants. This difference is the more pronounced for higher depolarizations: the τ_n^m/τ_n^s ratio amounts to 1.8 at a depolarization of 150 mV, but only to 1.2 at a depolarization of 70 mV.

DISCUSSION

The functional difference between sensory and motor nerve fibers is manifested in at least two major physiological phenomena: the shape of the action potential and the ability to fire repetitively under a sustained membrane stimulus. These differences may be due to differences in membrane properties, namely, membrane conductance and/or fiber structure. The results of this work indicate that there are definite differences in membrane conductance, and perhaps also differences in the perinodal structures.

TABLE III
THE TIME CONSTANT OF POTASSIUM CONDUCTANCE, τ_n, AS A FUNCTION OF MEMBRANE DEPOLARIZATION (V) IN MOTOR AND SENSORY FIBERS

Fiber type	V (mV)	
	+70	+150
	(*ms*)	(*ms*)
Sensory (7)	2.51 ± 0.09	0.52 ± 0.06
Motor (6)	3.07 ± 0.26	0.96 ± 0.06

The values are means ±SEM. Numbers in parentheses indicate number of fibers used for averaging. Fibers are same as those listed in Table II of Moran et al., 1980.

Perinodal Structures

The difference in potassium accumulation suggests a possible structural difference between motor and sensory fibers. Depending on the model accepted—the three-compartment model or the diffusion-in-an-unstirred-layer, DUSL, model—such a difference would be expected to be manifested in one of the following parameters: θ and P_{K_o} or D and l.

Within the framework of the first model, the apparent space thickness, θ, has been found to be almost twice as large in the motor as compared with the sensory fibers. In contrast, the apparent permeability of the external barrier, P_{K_o}, is similar in both types of fibers.

However, within the framework of the DUSL model, the two fiber types apparently do not differ; in either the values of the diffusion constant, D, or in those of the unstirred layer thickness, l.

The anatomical evidence, i.e., lack of obvious compartmentalization and the inconsistency of the space width with the basic assumption of instantaneous ion mixing (Moran et al., 1980) seem to indicate that the DUSL is perhaps the right model for the K accumulation in the node. As within the framework of this model, the two fiber types do not seem to differ in their perinodal structures, the differences in accumulation should probably be mainly attributed to differences in membrane potassium conductance systems.

Differences in Membrane Conductance

After correcting the error caused by K^+ accumulation (which is often significant) in the determination of the potassium chord conductance, G_K, (There is an effect of the accumulation process on the kinetics of G_K, i.e., an increase in its apparent rate of rise and consequently, a decrease in the experimentally determined τ_n.) marked differences are observed between the G_K systems of motor and sensory fibers. The absolute values of G_K have been found to be twice as large in sensory (1.1 S/cm^2), as compared with motor fibers (0.55 S/cm^2).

Different also is the G_{K_∞} dependency on membrane potential, which, for depolarizations >50 mV, is steeper in sensory fibers. This finding, observed here in accumulation corrected fibers bathed in normal Ringer's, is compatible with that of Bretag and Staempfli (1975) obtained using fibers bathed in isotonic KCl solutions, in which K^+ accumulation was assumed to be negligible.

The motor and sensory fibers also show a different gating kinetics, sensory fibers being progressively faster at strong depolarizations. Our values of τ_n (Table III) are compatible with the "half-times" ($t_{1/2}$) of potassium currents reported by the above authors, again in isotonic KCl. Note, however, that high external [K^+] was reported to slow the potassium conductance system in the node (Palti et al. 1976, Bengenisich, 1979). Thus, it seems that at least a major fraction of potassium channels is different in motor and sensory fibers.

The fact that for small depolarizations the G_{K_∞} vs. V_M curves of both preparations superimpose (Fig. 3 *A*), while at depolarizations above 60 mV, the "sensory" curve deviates from the "motor" curve, may indicate that both preparations contain the same "basic" channels, but that sensory fibers contain an additional population of channels. A similar interpretation has been adopted in the case of batrachotoxin treated sodium channels in the frog nodal membrane (Khodorov et al., 1975). This additional potassium channel population is activated only by relatively large depolarizations and is probably characterized also by faster kinetics (Table III).

The G_{K_∞} vs. V_M relationship of the basic population of channels (BPC) can be compared with that of the additional population of channels (APC). The BPC $G_{K_\infty} - V_M$ curve would be the motor fiber curve while the APC curve can be computed from the difference between the motor and sensory G_{K_∞} vs. V_M curves of Fig. 3 *A*. Fig. 5 illustrates such two curves, after a translocation of the APC curve by ~40 mV along the voltage axis in the hyperpolarizing direction. The two curves seem to be practically identical (note the size of the SEM bars in Fig. 3 *A*). The similarity between the two $G_{K_\infty} - V_M$ relationships of the two types of "channels" may be interpreted as an indication that the two types of units are basically similar except that the "voltage sensor" of one is biased by some 40 mV with respect to the other.

An alternative interpretation is that all "sensory" potassium channels are of one type, which is different from that of the "motor" channels.

One possible way to distinguish between these two alternatives would be to identify two conductance rate constants in a single currents response in the first case and only one in the second; however, this would not rule out the possibility of a single population with different kinetic schemes. Moreover, if in the first case the two populations of channels vary only by a "voltage sensor" bias, the $\tau_n - V_M$ relationship of the APC will be shifted with respect to that of the BPC by the same amount seen in Fig. 5 for the $G_{K_\infty} - V_M$ curves.

While the rate constants of motor and sensory fibers were found to be significantly different, it is difficult to identify an additional time constant in sensory fibers on top of τ_n and the kinetic effects of the potassium accumulation. However, in high K_o (80 mM) when the accumulation is minimal, a second, slower time constant does appear at strong depolarizations in sensory fibers.

The faster kinetics of the sensory potassium conductance system, measured at strong depolarizations, can probably account for the faster initial rate of repolarization (following the peak of the action potential) of sensory fibers. The rates of repolarization become similar only when V_M approaches resting values, where both the G_{K_∞} vs. V_M relationships and the τ_n values of motor and sensory fibers are practically identical. At this phase of the action potential the sensory G_K is either slightly lower than or equal to the motor G_K. Consequently, the phenomenon of repetitive firing, which is most probably due to a relatively higher G_{Na}/G_K ratio, during a sustained depolarizing stimulus, may only be slightly affected by the above

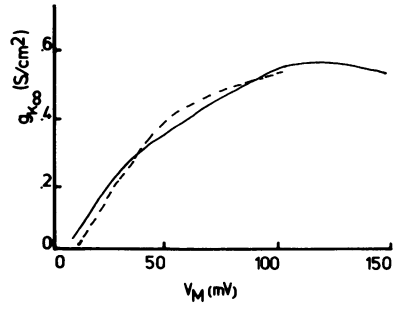

FIGURE 5 Steady-state potassium chord-conductance, g_{K_∞}, corrected for K^+ accumulation, as a function of membrane potential, V_M. Continuous line: average G_{K_∞} of seven sensory fibers, same as in Fig. 3 *A*; dashed line: the difference between sensory and motor G_{K_∞} values of Fig. 3 *A*, shifted by ~40 mV in the hyperpolarizing direction. Note the similarity in the two curves.

difference in the G_K systems. Since the leakage conductance was shown here to be similar to the two fiber types, the relative increased excitability of the sensory fibers should be attributed mostly to the G_{Na} system. In view of the correlation between the accommodation rate and the repetitive firing activity (Vallbo, 1964 *b*) the above is consistent with the suggestion of Vallbo (1964 *b*) and of Frankenhaeuser and Vallbo (1965) that the faster rate of accommodation in motor fibers (Vallbo, 1964 *a;* Schmidt & Stämpfli, 1964; Bergman and Stämpfli, 1966) results from increased sodium inactivation. Moreover, the reason these workers did not detect a significant difference between motor and sensory fibers in the effect of the potassium conductance on accomodation becomes clear in view of the fact that they studied accomodation only in the range of low depolarizations (under +50 mV), i.e., where we found the two G_K systems to be practically identical.

This work was supported in part by the Israeli National Academy of Sciences and by Deutsche Forschungsgemeinschaft Sonderforschungsbereich 38 "Membranforschung," and was done in partial fulfillment of the Doctor of Science degree for N. Moran.

Received for publication 10 December 1979 and in revised form 9 May 1980.

REFERENCES

BEGENISICH, T. 1979. Conditioning hyperpolarization induced delays in the potassium channels of the myelinated nerve. *Biophys. J.* **27**:257–266.

BERGMAN, C., and R. STAEMPFLI. 1966. Difference de permeabilite des fibres nerveuses myelinisees sensorielles et motrices a l'ion potassium. *Helv. Physiol. Pharmacol. Acta.* **24**:247–258.

BRETAG, A. H., and R. STAEMPFLI. 1975. Differences in action potentials and accomodation of sensory and motor myelinated nerve fibres as computed on the basis of voltage clamp data. *Pflügers Arch.* **354**:257–271.

DODGE, F. A. 1961. Ionic permeability changes underlying nerve excitation. *In* Biophysics of Physiological and Pharmacological Actions. American Association for the Advancement of Science, Washington, D.C.

DODGE, F. A. 1963. A study of ionic permeability changes underlying excitation in myelinated nerve fibers of the frog. Ph.D. Thesis. The Rockefeller University. University Microfilms (No. 64-7333), Ann Arbor, Michigan.

HILLE, B. 1973. Potassium channels in myelinated nerve. Selective permeability to small cations. *J. Gen. Physiol.* **61**:669–686.

KHODOROV, B. I., E. M. PEGANOV, S. V. REVENKO, and L. D. SHISHKOVA. 1975. Sodium currents in voltage clamped nerve fiber of frog under the combined action of batrachotoxin and procaine. *Brain Res.* **84**:541–546.

KOPPENHOFER, E. 1967. Die Wirkung von Tetraäthylammonium-chlorid auf die Membranströme Ranvierscher Schnürringe von Xenopus laevis. *Pflügers Arch.* **293**:34–55.

KOPPENHOFER, E., and H. SCHMIDT. 1968. Die Wirkung von Skorpiongift auf die Ionenströme des Ranvierschen Schnürring. I. Die Permeabilitaten P_{Na} und P_K. *Pflügers Arch.* **303**:133–149.

KOPPENHOFER, E., and H. SCHMIDT. 1968. Die Wirkung von Skorpiongift auf die Ionenströme des Ranvierschen Schnürring. II. Unvollstandige Natrium-Inactivierung. *Pflügers Arch.* **303**:150–161.

MORAN, N., Y. PALTI, E. LEVITAN, and R. STAEMPFLI. 1979. Potassium ion accumulation at the axolemmal surface of the nodal membrane in frog myelinated fibers. *Biophys. J.* **32**:939–954.

NONNER, W. 1969. A new voltage clamp method for Ranvier nodes. *Pflügers Arch.* **309**:116–192.

NONNER, W., E. ROJAS, and R. STAEMPFLI. 1975. Displacement currents in the node of Ranvier, voltage and time dependence. *Pflügers Arch.* **354**:1–18.

PALTI, Y., G. GANOT, and R. STAEMPFLI. 1976. Effect of conditioning potential on potassium current kinetics in the frog node. *Biophys. J.* **16**:261–273.

SCHMIDT, H., and R. STAEMPFLI. 1964. Nachweis unterschiedlicher electrophysiologischer Eigenschaften motorischer und sensibler Nervenfasern des Froshes. *Helv. Physiol. Pharmacol. Acta.* **22**:C143–C145.

SCHMIDT, H., and R. STAEMPFLI. 1966. Die Wirkung von Tetraäthylammonium chlorid auf den einzelnen Ranvierschen Schnürring. *Pflügers Arch.* **287**:311–325.

STAEMPFLI, R. 1969. Dissection of single nerve fibres and measurement of membrane potential changes of Ranvier nodes by means of the double air gap method. *In* Laboratory Techniques in Membrane Biophysics. H. Passow and R. Staempfli, editors. Berlin-Heidelberg-New York, Springer-Verlag, Berlin. 157–166.

STAEMPFLI, R., and B. HILLE. 1976. Electrophysiology of the peripheral mylelinated nerve. *In* Frog Neurobiology. R. Llinas and W. Precht, editors. Springer-Verlag, Berlin.

VALLBO, Å. B. 1964 *a*. Accommodation of single myelinated nerve fibers from *Xenopus laevis* related to type of end organ. *Acta Physiol. Scand.* **61**:413–428.

VALLBO, Å. B. 1964 *b*. Accommodation related to inactivation of the sodium permeability in single myelinated nerve fibers from *Xenopus laevis*. *Acta Physiol. Scand.* **61**:429–444.